

Fatigue Failure Analysis in AISI 304 Stainless Wind Turbine Shafts

M. F. V. Montezuma, E. P. Deus, M. C. Carvalho

Abstract—Wind turbines are equipment of great importance for generating clean energy in countries and regions with abundant winds. However, complex loadings fluctuations to which they are subject can cause premature failure of these equipment due to the material fatigue process. This work evaluates fatigue failures in small AISI 304 stainless steel turbine shafts. Fractographic analysis techniques, chemical analyzes using energy dispersive spectrometry (EDS), and hardness tests were used to verify the origin of the failures, characterize the properties of the components and the material. The nucleation of cracks on the shafts' surface was observed due to a combined effect of variable stresses, geometric stress concentrating details, and surface wear, leading to the crack's propagation until the catastrophic failure. Beach marks were identified in the macrographic examination, characterizing the probable failure due to fatigue. The sensitization phenomenon was also observed.

Keywords—Fatigue, sensitization phenomenon, stainless steel shafts, wind turbine failure.

I. INTRODUCTION

UNLIKE large wind power stations, small wind turbines are in areas, often residential or industrial, where there is easy access for people. In Northeast Brazil, a region with constant and abundant winds, wind energy is a good option for clean energy for small consumers interested in adopting the energy compensation system. However, failures in this equipment's components can cause catastrophic accidents, being a significant risk to human lives.

Although a considerable number of studies have been dedicated to the detection of wind turbine failures, there are still many unresolved problems, due to the complexity of the system and the reliability of the installed sensors. Most of these studies, however, focus on the detection of failures in the turbine blades, gearboxes, and bearings [1], [2]. However, the main shafts are one of the key components (see Fig. 1), as they absorb loads from the hub, being responsible for the transfer of the mechanical energy generated by the turbine to an electric generator, according to the schematic drawing in Fig. 1.

M. F. V. Montezuma is with the Department of Metallurgical and Materials Engineering, Federal University of Ceará, Technology Center, Pici Campus Street, CEP 60440-554 - Fortaleza, CE, Brazil (phone: +55-85-981681914; e-mail: marcosmontezuma@alu.ufc.br).

E. P. Deus is with the Department of Metallurgical and Materials Engineering, Federal University of Ceará, Technology Center, Pici Campus Street, CEP 60440-554 - Fortaleza, CE, Brazil (phone: +55-85-99710608; e-mail: epontes@ufc.br).

M. C. Carvalho Lorena School of Engineering, University of São Paulo, Campinho Municipal Road, New Bridge, CEP 12602-810 - Lorena, SP, Brazil (phone: +55-91-992386710; e-mail: marciocorreia@usp.br).

Failure studies carried out on wind turbine shafts [3] showed that the main reasons that resulted in the fracture of the main shaft were stress concentration on the shaft surface near the critical section, caused by the diameter changes, the lack of homogeneity of the microstructure and surface defects, combined with the condition of variable loads to which they are subjected, causing the fatigue failure process.

Although the wind turbines have an estimated life of 20 years, some wind turbines failed to operate prematurely, where AISI 304 stainless steel shafts were catastrophically broken. This work aims to study the failure that occurred in AISI 304 stainless steel shafts used in small wind turbines so that it serves as a contribution to avoid similar problems.

In this work, six shafts were used in two different models of wind turbines. First, macrographic analyzes were carried out to verify the origin of the failures. A micrographic analysis was carried out to identify possible discontinuities or micro failures that justified reducing the component's useful life. The causes that led to the failure (metallurgical defects, surface wear, geometric concentrator) were studied.

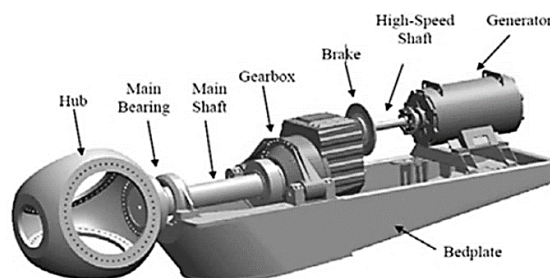


Fig. 1 Schematic drawing of parts of a wind turbine

II. MATERIALS AND METHODS

Six AISI 304 stainless steel shafts used in two different wind turbine models were analyzed.

The methodology used in this work was based on the visual inspection of the fractured part with digital images captured by digital cameras, scanning electron microscopy, chemical analysis using EDS, hardness testing, and metallographic analysis. The shafts were cut into smaller parts for the macro and micrographic analysis of the fracture and the materials' chemical and hardness analysis. The specifications of these models of wind turbines and sample identification are shown in Table I.

Figs. 2 and 3 show the parts as received, the motivating shafts of the analysis, and the failure region, differentiated according to the manufacturer.

TABLE I
SPECIFICATIONS OF THE A3300 AND A1700 WIND TURBINE MODELS

Power	3300 W (MODEL A3300)	1700 W (MODEL A1700)
Voltage	110/220 V – 50/60Hz	110/220 V – 50/60Hz
Rotor diameter	5920 mm	3870 mm
Blade	Fiberglass	Fiberglass
Blade size	2930 mm	1900 mm
Tower	20 m	20 m
Weight	147.0 kg	83.5 kg
Power	Inverter 180-260 V, 50/60 Hz	Inverter 180-260 V, 50/60 Hz
Inverter	SMA Wind Boy WB3800	SMA Wind Boy WB3300
Braking system	Disc brake with electromagnetic drive (both)	
Estimated service life	Disc brake with electromagnetic drive (both)	
Sample identification	I B1 B2	PP AP RA

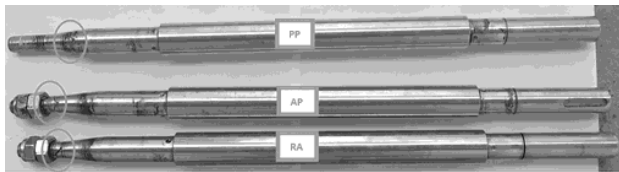


Fig. 2 Wind turbine shafts - Model A1700



Fig. 3 Wind turbine shafts – Model A3300

Before the shafts were cut to take samples, a thorough visual inspection of the fractured parts was carried out, with digital images (captured by digital cameras) to be kept as a record and, later, used for macroscopic analysis. Subsequently, the shafts were cut using a hand saw to fit the micrographic analysis equipment. After the cuts, the parts were analyzed using a Scanning Electron Microscope.

After completing the fractures' macro and microscopic analysis, some standard sample preparation procedures were performed for the metallographic analysis [4], and the samples were etched with Nital for optical microscopy analysis.

III. RESULTS AND DISCUSSIONS

Four different types of failures were observed in the visual analysis: two shafts fractured in the thread region (I and B1) and two at the beginning of the thread (RA and AP); two shafts showed flaws in the tapered region of the axis (PP and B2).

In the visual analysis, different failures morphologies were observed and compared with Metals Handbook [5]. The generator shafts A1700 - AP and RA broke at the beginning of the thread, Fig. 4, with fatigue break marks shown in detail in Figs. 5 and 6.

It is important to note that the images presented in this work, Figs. 2-4, and 9, were taken after the macro and

micrographic analysis of the fracture surfaces, so that the coupling of the surfaces did not impair the interpretation of the failed analysis results.

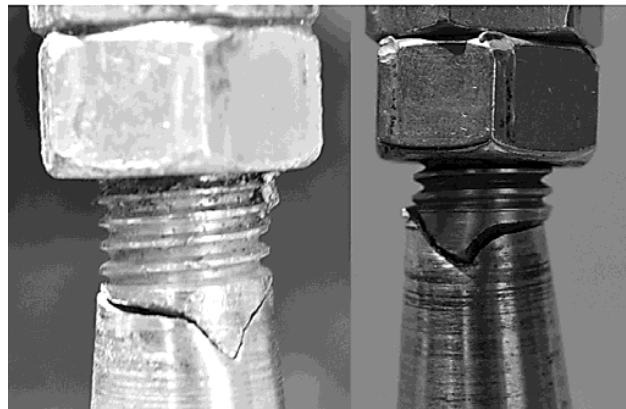


Fig. 4 AP and RA fractured shafts - Model A1700

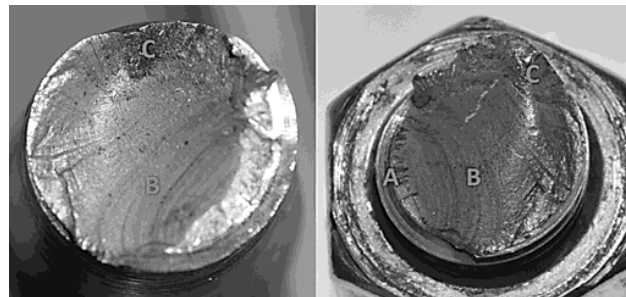


Fig. 5 View of the fatigue fracture region of the RA shaft: A - beginning of the fracture, B - beach marks, and C - final region of the fracture

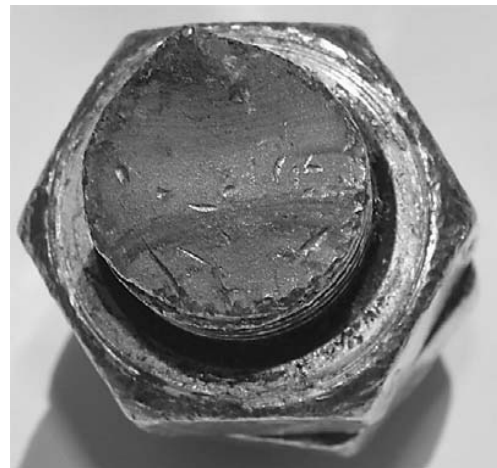


Fig. 6 View of the fatigue fracture region of the AP shaft – verification of beach marks

The visual inspection of the fracture on the AP shaft was compromised due to the numerous tool marks in the fracture regions, Fig. 6. However, it was possible to observe the "beach marks" characteristic of fatigue fracture.

Two shafts of the A3300 wind turbine (I and B1) broke in the first thread in contact with the nut or locknut, as shown in Figs. 7 and 8.

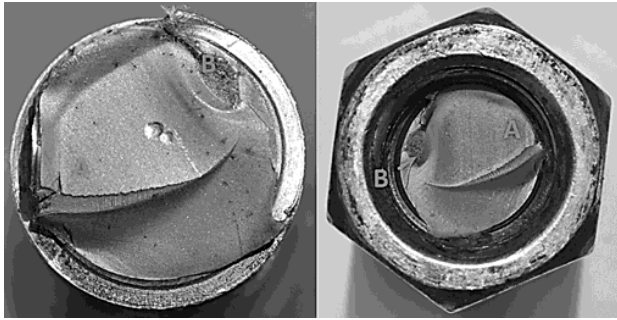


Fig. 7 View of the fatigue fracture region of the shaft I - Model A3300

The shaft I surface observed in Fig. 7 presented a region with a smooth aspect (A), corresponding to the area over which the crack spread slowly, and the smaller area (B) with a fibrous texture corresponds to the region the failure occurred. Quickly (catastrophic), which characterizes a fatigue failure.

The B1 shaft, Fig. 8, presented two different types of fracture surface. On the right side, smooth surface (A), there is the fatigue zone, while on the other end, rough surface (B), the plastic zone is characterized by the appearance of tearing.

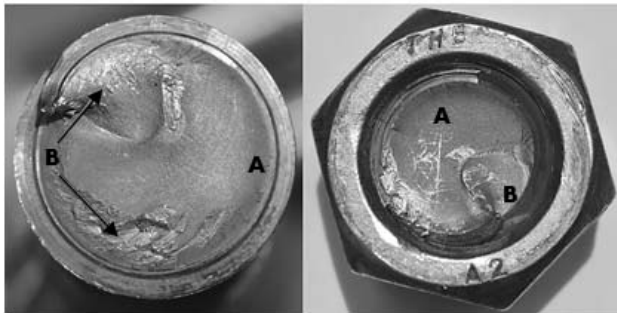


Fig. 8 View of the fatigue fracture region of the B1 shaft - Model A3300

A superficial wear is visible on the PP axis of the A1700 wind turbine, where the part broke in the tapered transition region, favoring the initiation and propagation of cracks and fatigue failure, Fig. 9.

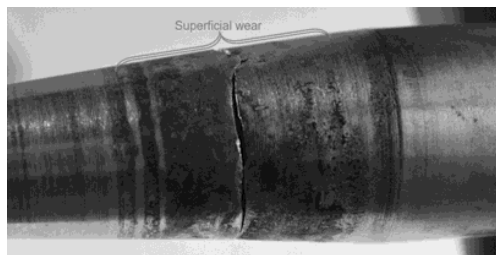


Fig. 9 View of the superficial wear on the fracture region of the PP axis - Model A1700

The fracture surface of the PP shaft can be seen in Fig. 10. Point A indicates the beginning of the crack that has spread, leaving "beach marks," indicated by point B and finally point C indicating the final region of the fracture. The fracture or rupture of the material usually occurs with the formation and propagation of a crack that begins at points where there is structural or compositional imperfection or a high-stress concentration, which generally occurs on the surface, as presented in the piece, where the wear marks and the consequent oxidation generated stress concentrating points. The darker coloration at point A shows oxidation and infiltration of contamination during the fracture's relatively long propagation stage.

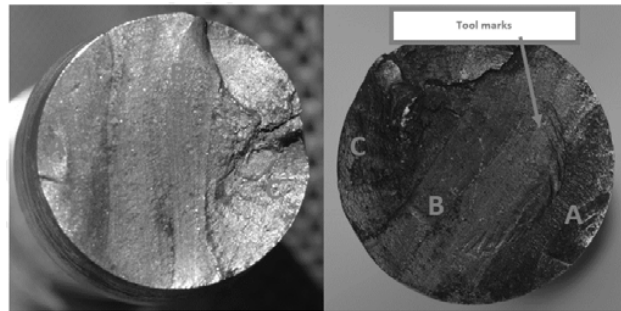


Fig. 10 View of the fatigue fracture surface of the PP axis - Model A3300

Similar wear was also observed in the B2 axis of the A3300 wind turbine, Fig. 11, and the other axes, however, with less intensity.

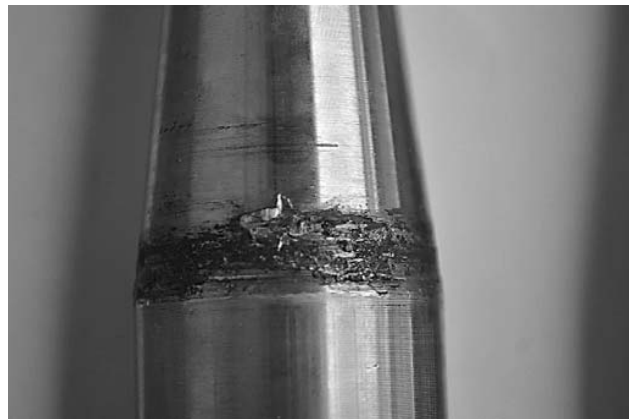


Fig. 11 Critical region of axis B2, due to loss of material due to wear (contact marks) and oxidation - Model A3300

Samples taken from the fractured regions were analyzed in the Scanning Electron Microscope (SEM).

Secondary cracks were observed in all faults and the B1 axis, inclusions, and porosity. Secondary cracks in early growth stages are associated with grain boundaries, sliding bands, and skin contours, regardless of the test medium. In [6], the number of secondary cracks increases with the increase in the level of stress and the aggressive medium. However, the

porosity found in the B1 axis demonstrates a possible manufacturing problem, since the presence of gases dissolved in the metal liquid can result both in the presence of various types of oxide inclusions, as well as in the formation of porosities of endogenous origin, that is, metallurgical causes, inherent to the quality of the metal cast in the molds. There are also exogenous origin defects originating from external causes, such as molds and leakage and feeding channel

systems [7].

For the pieces' chemical characterization, samples analyzed in metallography were used, and an optical emission spectrometer measured the composition. The measured values of the specific elements are shown in Table II. According to the EDS results, it was possible to verify that the shafts presented values consistent with the stainless steel AISI 304.

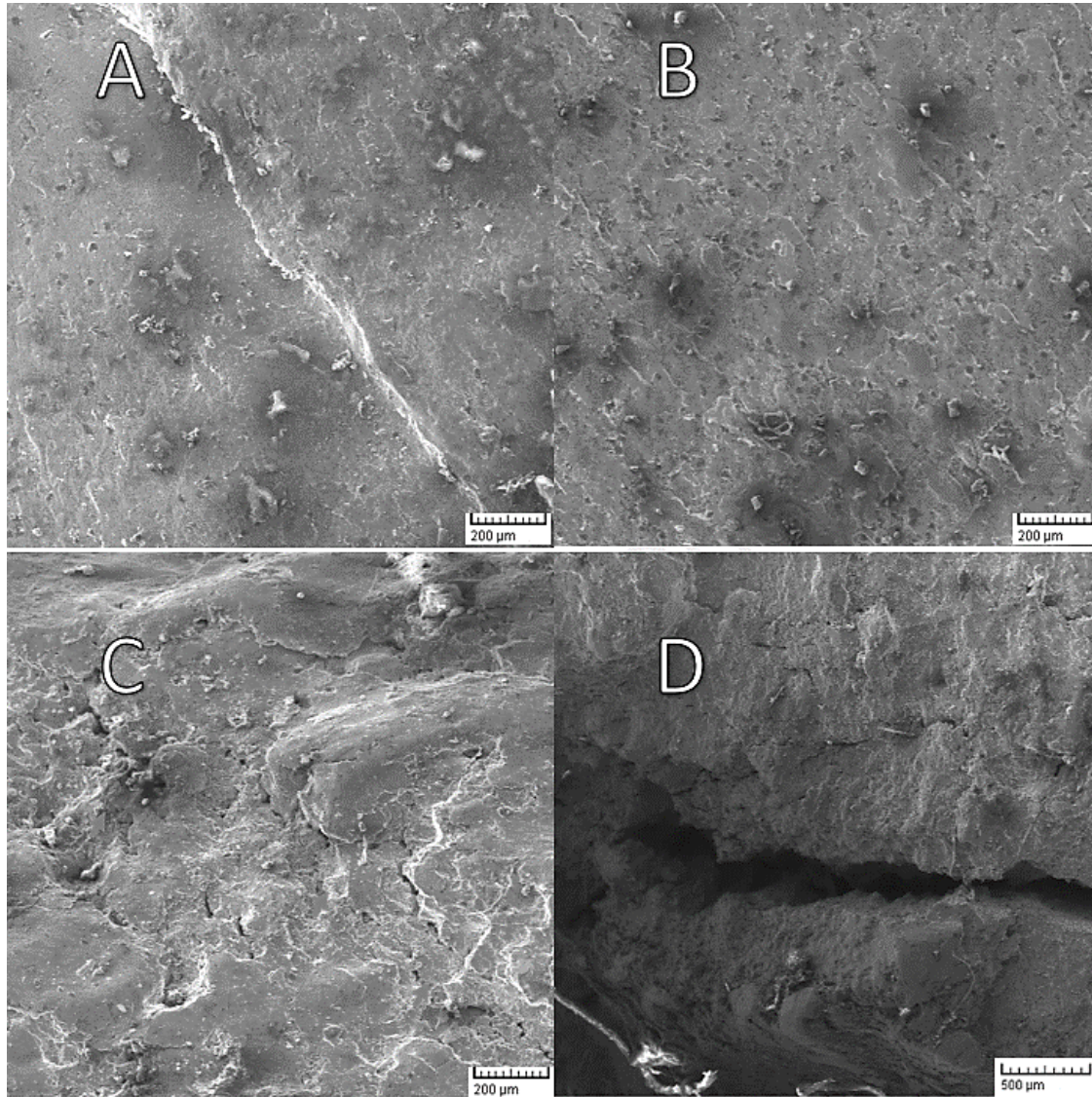


Fig. 12 SEM of the fractured region of the PP axis: A - region of the beginning of the failure, B - a region of the beach marks, C - a region of the catastrophic fracture with several secondary cracks, and D - secondary crack highlighted

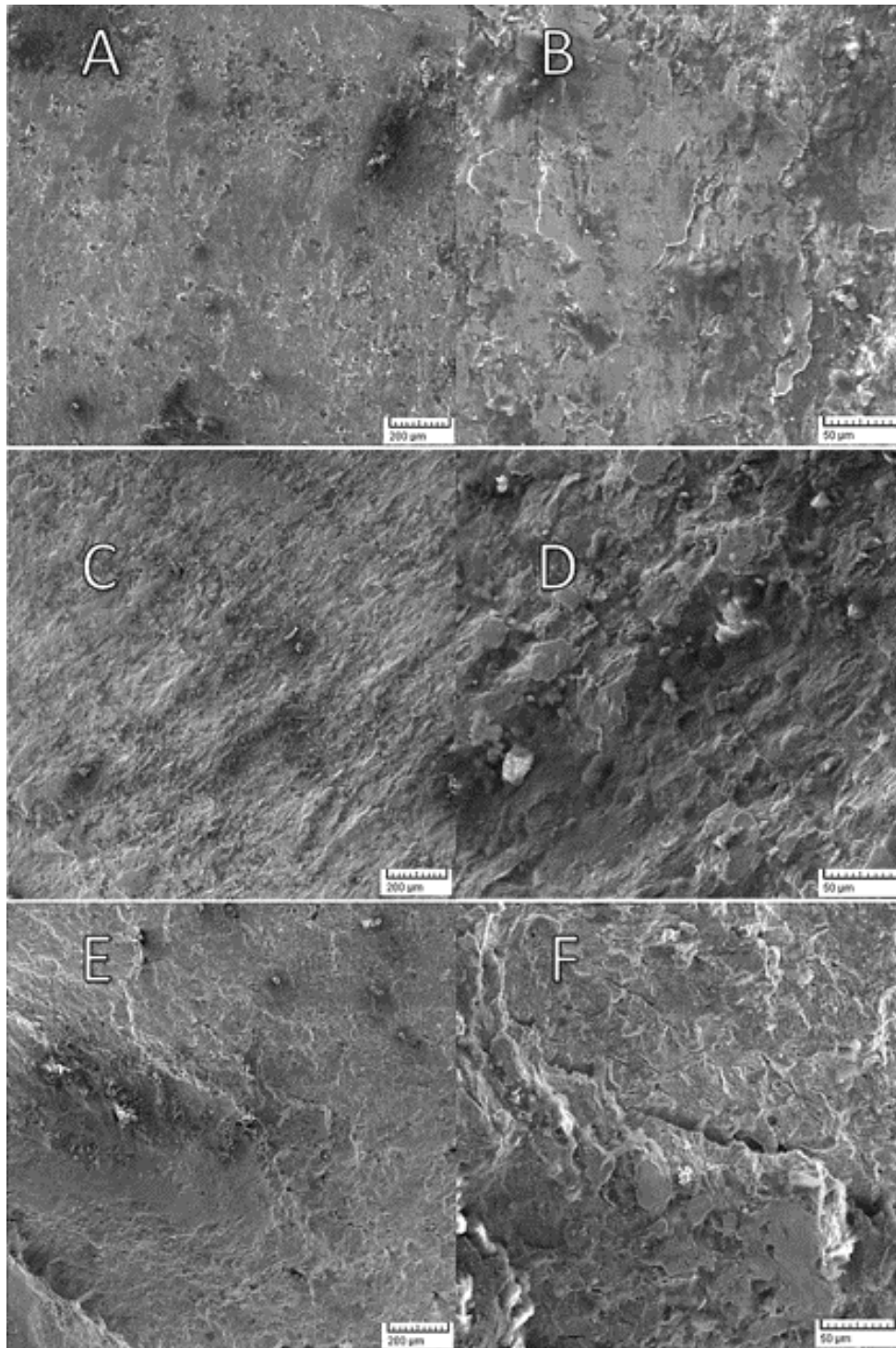


Fig. 13 SEM of the fractured region of the AP axis: A - a region of the beginning of the fatigue failure, B - detail of the region of fatigue in which the crack propagated slowly, C - a region of the beach marks, D - fatigue striation, high rate of deformation, E - catastrophic fracture region with secondary cracks and F - secondary crack highlighted

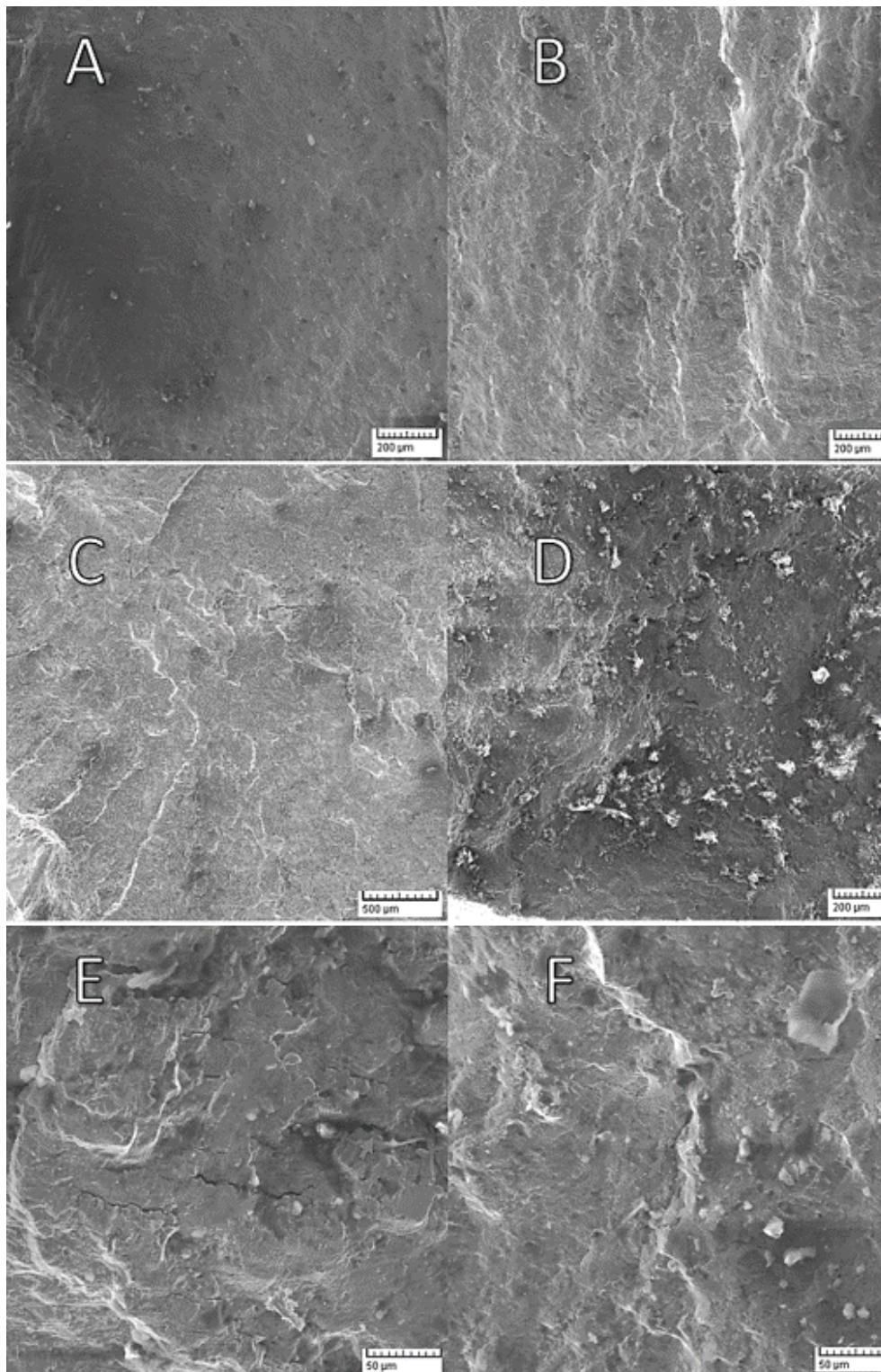


Fig. 14 SEM of the fractured region of the RA axis: A - region of the beginning of the fatigue failure, B - detail of the region of fatigue in which the crack spread slowly, the appearance of beach marks, C- a region of beach marks, D - region beginning of catastrophic fracture, the appearance of secondary cracks, E and F - regions of catastrophic fracture with secondary cracks

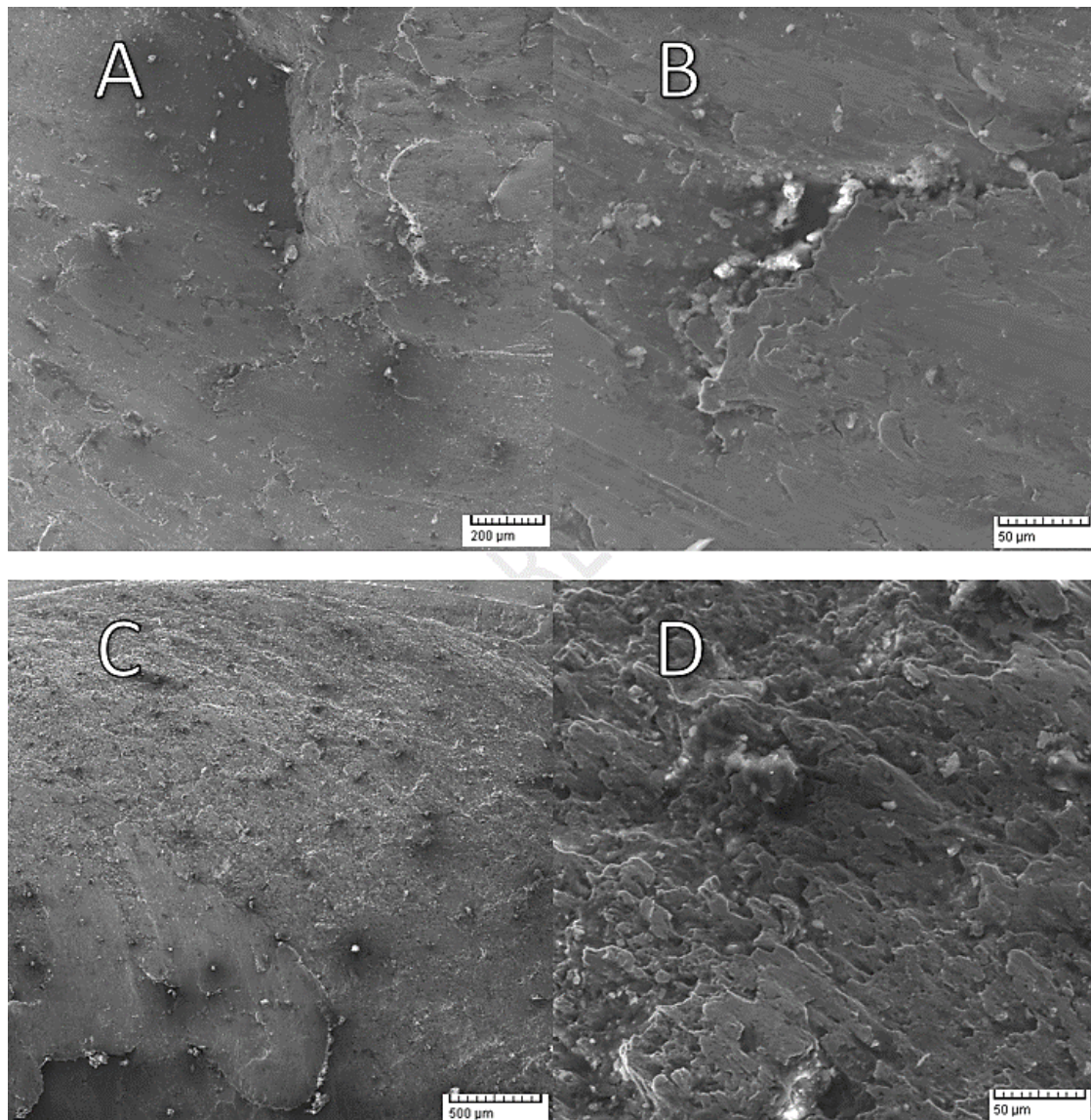


Fig. 15 SEM of the fractured region of axis I: A - region of the beginning of the fatigue failure, B - detail of the region of fatigue in which the crack propagated slowly, C - a region of slow/catastrophic failure transition D - a region of the catastrophic fracture

TABLE II
RESULT OF CHEMICAL ANALYSIS (WT%)

	Cr	Fe	Mn	Ni	C	Si
Standard AISI 304	18.09	Rest.	1.31	8.03	0.06	0.39
Results	20.47	72.80	-	8.42	-	-

The hardness test was performed on the Rockwell - B scale. They result in an average of 55HRB and 60HRB for the materials used on the axes of the A1700 and A3300 wind turbines. The values found were lower than those specified for stainless steel AISI 304, whose reference value is 80 to 85 HRB, were expected due to the high deformation suffered in

the microstructure of this region.

The structure of austenitic steel (stainless steel) with chromium-rich carbides precipitation was observed in the grain boundary region. This type of steel becomes susceptible to intergranular corrosion due to the phenomenon of sensitization, which is a process related to the precipitation of chromium-rich carbides in the grain boundary region, leaving the adjacent region depleted of chromium [8].

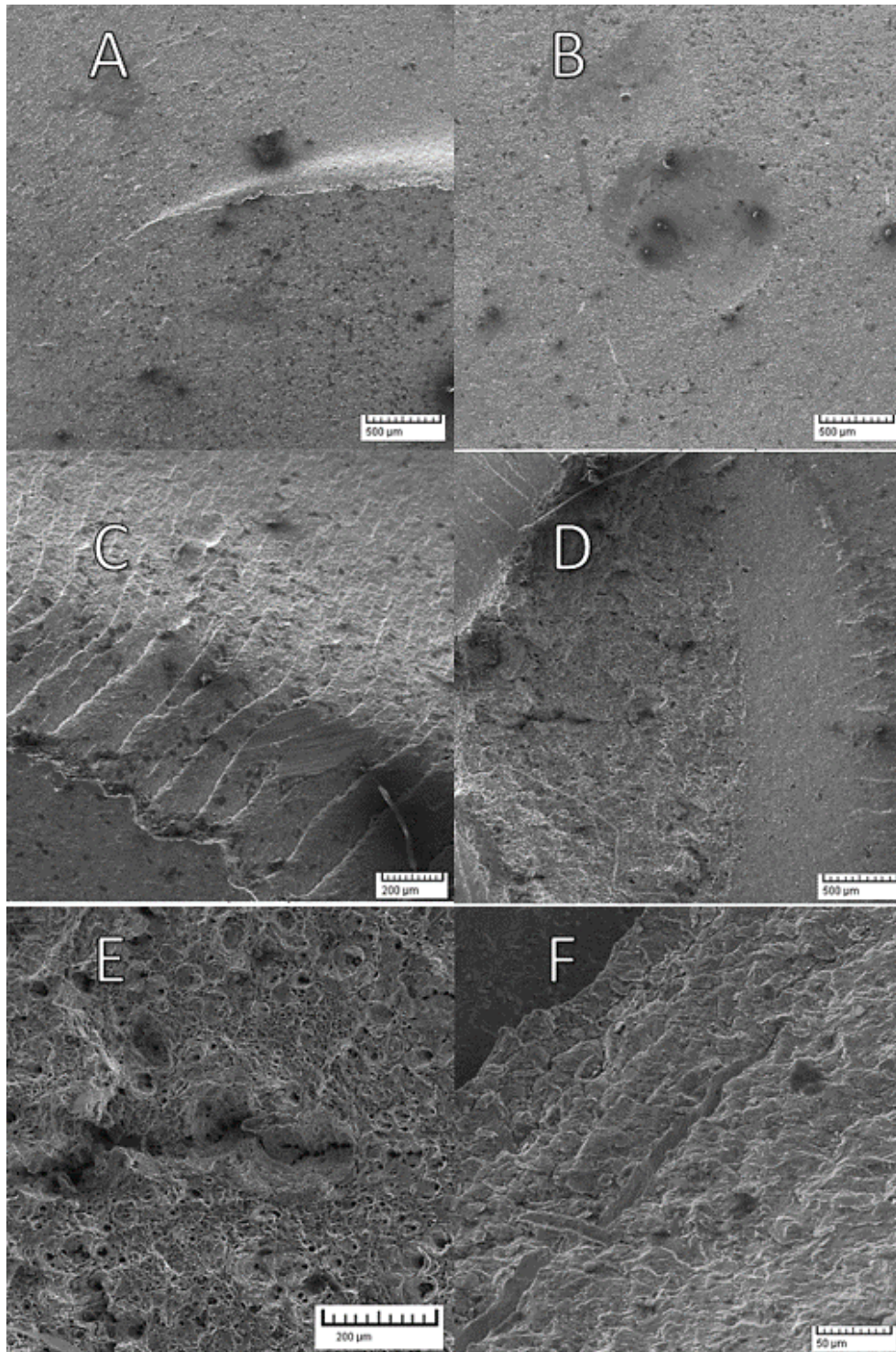


Fig. 16 SEM of the fractured region of the B1 axis: A - region of the beginning of the fatigue failure, B - Inclusions, C - beach marks, D - a region of the beginning of the catastrophic fracture, the appearance of secondary cracks, E - secondary cracks and porosity and F - secondary crack

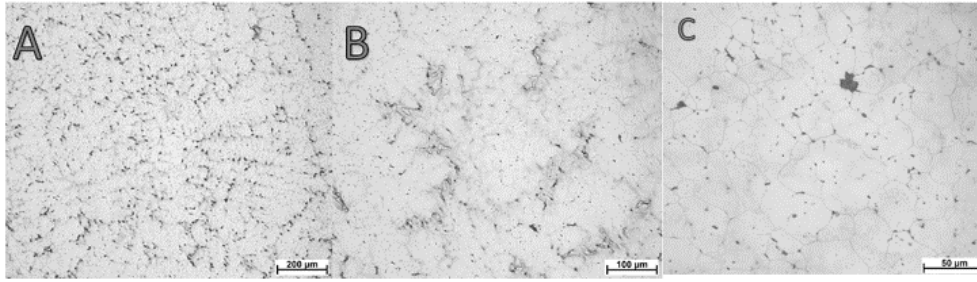


Fig. 17 Metallographic samples of the material

IV. CONCLUSIONS

USA, 1996

According to the results obtained, presented, and discussed in this work, we observed that metallurgical defects (sensitization), and a region with undesirable wear due to contact were detected, causing stress concentrators that, together with variable stress levels, reduce the life of the part, failing due to fatigue.

The results from morphological, chemical, and metallographic analyzes demonstrate that the material used in the manufacture of the shafts is from the family of austenitic stainless steels which, according to the chemical composition, is an AISI 304 treated by recrystallization, an annealing process applied to cold-processed metals for obtaining nucleation and growth of new grains without changing the phase. This heat treatment allows the recovery process by reducing or eliminating the hardening processes (stresses), decreasing the hardness, and increasing the ductility. However, this process favors sensitization, a phenomenon that favors the formation of microscopic cracks along the grain boundaries of the material's metallurgical structure, with virtually no change in the piece's dimensions. When the cracks reach a certain depth, the piece may break, or pieces of material may become detached due to mechanical efforts, even very low, a situation verified in all the pieces.

REFERENCES

- [1] J. C. Marín, A. Barroso, F. París, J. Cañas, Study of fatigue damage in wind turbine blades, *Eng. Fail. Anal.* 16 (2009) 656–668. <https://doi.org/10.1016/j.engfailanal.2008.02.005>.
- [2] M. H. Evans, A.D. Richardson, L. Wang, R.J.K. Wood, Serial sectioning investigation of butterfly and white etching crack (WEC) formation in wind turbine gearbox bearings, *Wear.* 302 (2013) 1573–1582. <https://doi.org/10.1016/j.wear.2012.12.031>.
- [3] Z. Zhang, Z. Yin, T. Han, A.C.C. Tan, Fracture analysis of wind turbine main shaft, *Eng. Fail. Anal.* 34 (2013) 129–139. <https://doi.org/10.1016/j.engfailanal.2013.07.014>.
- [4] ASTM E3:11, Standard Guide for Preparation of Metallographic Specimens, 2017.
- [5] M. Handbook, *Metals Handbook: Fractography and Atlas of Fractographs*, First Edit, American Society for Metals, 1974.
- [6] E. J. Giordani, V. A. Guimarães, T. B. Pinto, I. Ferreira, Study of the nucleation mechanisms of fatigue cracks and fatigue-corrosion of ASTM F 138 stainless steel used as biomaterial, *Brazilian Congress of Materials Science and Engineering – CBECIMAT*, 2550-2557, Natal, RN, Brazil, 2002.
- [7] F. L. Fachini, Deoxidation study of CF8M stainless steel (AISI 316) in a conventional induction furnace, with variable additions of CaSi and CaSiMn, Master's Dissertation in Mechanical Engineering – Superior Institute Tupy, 51p. Joinville, SC, Brazil, 2009.
- [8] A. J. Sedriks, *Corrosion of Stainless Steels*, Second Edi, New York,